John C. Munday, Jr.
Paul L. Zubkoff
Virginia Institute of Marine Science
College of William and Mary
Gloucester Point, VA 23062

Remote Sensing of Dinoflagellate Blooms in a Turbid Estuary

Only limited accuracy is possible because simultaneous variations in chlorophyll and inorganic suspended sediment concentrations can allow equivocal reflectance changes.

Abstract: *Dinoflagellate blooms in sediment-laden waters of the York River, Virginia consistently produced reflectance decreases in visible bands, but produced equivocal changes in the photographic infrared. The equivocal infrared changes are due to simultaneous variations in chlorophyll and inorganic suspended sediment concentrations, as interpreted with a reflectance model. Equations are developed to show what conditions of changing chlorophyll and sediment can produce invariant reflectance. Color photography of dinoflagellate blooms in turbid estuaries portrays chlorophyll distributions with limited accuracy. The complexity of the spatial distributions necessitates remote sensing for synoptic mapping.*

Introduction

Summer blooms of the dinoflagellates *Gymnodinium splendens* and *Cochlodinium heterolobatum* ("Red Water") have been reported for several years in the York River, Virginia and other estuaries contiguous with the lower Chesapeake Bay (Zubkoff *et al.*, 1975, 1979). Blooms in 1975-1977 were studied with aerial photography and extensive surface data collection; the 1978 bloom was photographed weekly over an eight-week period. The photographs reveal complex spatial patterns of surface phytoplankton abundance which appear to portray hydrodynamic processes. From the photographs and surface sampling, coarse quantitative estimates have been made of chlorophyll biomass for areas several kilometres long.

It would be desirable to prepare accurate maps of chlorophyll concentration and phytoplankton abundance using photographic or other remote sensing data. Oceanic chlorophyll measurement by remote sensing advanced considerably during the 1970s (see, for example, Gordon and Brown, 1973; Mueller, 1973; Duntley *et al.*, 1974; McNeil *et al.*, 1976; Morel and Prieur, 1977; Wilson and Kiefer, 1979). In estuaries, reports have indicated that infrared band (700 to 800 nm) remote sensing will portray estuarine phytoplankton blooms for chlorophyll concentrations above 10 to 30 $\mu g/l$ (Bressette, 1973; Bressette and Lear, 1973; Bukata *et al.*, 1974; Scherz, 1977). We therefore investigated the feasibility of extracting chlorophyll concentrations from bloom data and photographs. From the data and from results of reflectance model simulations, we find that only limited accuracy is possible, because simultaneous variations in chlorophyll and inorganic suspended sediment concentrations can allow equivocal reflectance changes. Thus, in a turbid estuary, the remote sensing of chlorophyll and phytoplankton will be more difficult than in oceans and large, clear lakes, due to hydrodynamic factors and to the greater abundance and diversity of suspended constituents, both living and nonliving.

Methods

The York River is a polyhaline estuary 50 km long terminating in the Chesapeake Bay. The

Photogrammetric Engineering and Remote Sensing,
Vol. 47, No. 4, April 1981, pp. 523-531.

width of the lower York averages 3 km. Average depth in the lower York channel is 12 m, the tidal amplitude averages 1 m, surface salinities between April and September range from 10 to 25‰, and temperatures range from 12 to 28°C (Zubkoff *et al.*, 1979). Secchi depths range from 0.5 to 2 m.

Nadir photographs in 35-mm, 70-mm, and 229-mm (9-inch) format were taken at 600 to 1600 m flying heights during mid-day under generally clear skies when blooms were highly visible. Color reversal films included Kodak Ektachrome 200, Aerochrome 2448, Hi-Speed Ektachrome, and Aerochrome Infrared 2443, with permutations of haze, light yellow, deep yellow, and red filters; most photography utilized a color film and haze filter. Photographic densities after commercial processing were measured with a Brumac color densitometer (diffuse density; 1 mm diameter circular aperture) and a Joyce-Loebl scanning microdensitometer (specular density; 200 by 200 μm square aperture). Calibration was by means of a silver-grain emulsion Kodak step wedge, which allows wavelength-dependent scattering and thus is suitable only for diffuse density calibration. Therefore, the results are only relatively calibrated. Color separation on the Joyce-Loebl was accomplished with Kodak Wratten filters 92, 93, and 94. In photographic density analysis using these filters, there is the possibility of density "spillover" from one color separation band to another due to overlap of the spectral absorbance curves of the emulsion layer dyes after processing (Scarpace, 1978). Spillover was found to be negligible because density changes in one band as large as 0.18 failed to record in other bands when the density noise level was 0.01.

Sampling from small craft was usually limited to vertical profile data, but on occasion surface sampling directed from the aircraft via radio was simultaneous with aerial photography, as required for proper photo calibration. Surface samples were obtained from the upper 0.3 m. Chlorophyll *a* concentrations corrected for phaeophytin were determined by filtration, extraction, and fluorometry (Strickland and Parsons, 1972) and suspended sediment concentrations by a gravimetric technique. All filtration was with 0.45 μm pore-size filters. Inorganic and organic sediment fractions were partitioned by means of ashing. Dinoflagellate absorption spectra were obtained with a Cary 15 spectrophotometer using the wet-filter technique of Govindjee (1960).

Data and Observations

Aerial reconnaissance

The usual basis for a decision to photograph a phytoplankton bloom was the appearance of "Red Water" as seen from the air or surface. The resulting photographs reveal colors notably different from those seen in the field (differences could be expected due to the difference between photographic and visual mechanisms). Visually, from the surface and from the air, *G. splendens* blooms appeared red-maroon, but on Ektachrome film (plus haze filter) and Aerochrome infrared film (plus Wratten 15 yellow filter) they were purple-black. *C. heterolobatum* was visually dark amber, and on Ektachrome film amber-black. The respective absorption spectra obtained from field samples are shown in Figure 1. Absorption by *G. splendens* is relatively weaker than absorption by *C. heterolobatum* between 450 nm and 650 nm. Furthermore, the colors recorded on film appeared washed out and the contrast between "Red Water" and clear water was less obvious than seen in the field. Consequently, it was sometimes difficult to identify "Red Water" on the photographs, even if visual detection from the air had appeared certain or a bloom was confirmed by direct analysis of the water column.

Aerially-directed sampling was successful in providing a wide range of surface chlorophyll *a* concentration (C) values. Broad intervals of C could be visually discriminated from the air: "clear" water ($C < 50$ μg/l), "intermediate" bloom water ($50 < C < 100$), and "dense" bloom water ($C > 100$). The data show that "clear" water was usually quite turbid, and had C values considerably greater than the York River background levels of 4 to 20 μg/l (Zubkoff and Warinner, 1976). Thus, York River blooms with $C \sim 50$ μg/l can escape visual detection when the background turbidity is high.

Chlorophyll and suspended sediment data for photo calibration

Chlorophyll *a* and suspended sediment data at six locations in the *C. heterolobatum* bloom on 18 September, 1978 were precisely synchronized

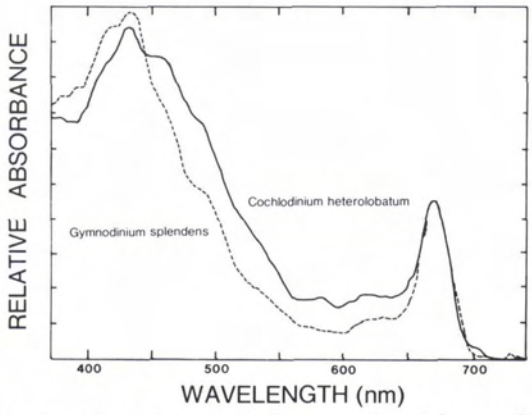

Fig. 1. Absorption spectra from samples of blooms of *Gymnodinium splendens* and *Cochlodinium heterolobatum*. Normalized at 680 nm.

with photography which pictured the sampling vessel near the frame centers. The chlorophyll *a* concentrations (C) ranged from 19 to 1038 μg/l, and the total suspended sediment concentrations (S) ranged from 14 to 212 mg/l. For $C = 1038$ μg/l, the organic (S_0) and inorganic (S_i) fractions were, respectively, 48 and 32 mg/l. The Pearson correlation coefficient (r) between C and S_0 is $r = 0.83$ ($p < 0.05$), and for C and S_i, $r = 0.0005$.

IMAGE INTERPRETATION AND DENSITOMETRY

On positive color and color-infrared transparencies (panchromatic copies are shown in Figure 2), regardless of the filter used, dense concentrations of dinoflagellates appear visually dark against a visually-bright turbid-water background. Densitometry confirmed that, in regions of heavy dinoflagellate concentrations, color film images show density increases corresponding to reflectance decreases. These reflectance decreases occur in all three Ektachrome spectral bands (400 to 500 nm, 500 to 600 nm, and 600 to 700 nm). The largest changes are in the blue band. For the 18 September data, r values between ln C and the blue, green, and red band densities were, respectively, 0.77, 0.77, and 0.65 (vignetting and other corrections neglected).

In the color-infrared transparencies, dense cell concentrations usually appear dark, but in addition there are a few areas of light pink coloration. These were studied by scanning microdensitometry, as in Figure 3. Here the scans traverse boat wakes, naturally-occurring zones of high and low cell concentration, a foam line, and an adjacent pink area. The pink coloration is caused by high cell concentrations converging at the foam line, which produce an infrared reflectance increase (Bressette, 1973; Bressette and Lear, 1973; Bukata *et al.*, 1974; Scherz, 1977). The foam line and the pink area can be distinguished on the scans: the foam line causes a narrow peak in the scans of the green (500 to 580 nm) and red (580 to 680 nm) bands, while in the infrared band (680 to 850 nm), the peak is broader and offset from the foam line position. Conversely, zones not visibly pink but still having high dinoflagellate concentrations (as determined from green and red band densities and spatial patterns) show small reflectance decreases. Boat wakes which break apart dense cell layers at the surface produce reflectance increases. Thus, in the infrared band, high cell concentrations are sometimes accompanied by a reflectance increase (pink areas) and at other times by a reflectance decrease (non-pink areas of high cell density).

The green and red bands of Aerochrome Infrared 2443 film behave similarly to color film bands, showing reflectance decreases in regions of high cell concentrations. Only the infrared band shows equivocal reflectance changes.

The coordinated photography and sampling permits estimates of chlorophyll spatial density on the York River during pronounced blooms. Based on photography calibrated by means of densitometry with surface and vertical profile chlorophyll measurements, chlorophyll *a* in September 1978 reached a spatial density of 100 kg/km^2 (a total of 2 metric tons for the lower York River), compared to nonbloom values of 4 to 20 kg/km^2.

ANALYSIS

PATCHINESS AND REMOTE SENSING

The striking feature of all the photography is the complexity of dinoflagellate distribution (see Figure 2). Mechanisms affecting distribution include tidal cycles, monthly hydrodynamic cycles (Haas, 1977), seasonal estuarine circulation cycles (Tyler and Seliger, 1978), nutrient levels, insolation, and cell motility. Sequences of photography show that dinoflagellate distributions change hourly during tidal cycles and that small-scale patchiness is ubiquitous and rapidly varying in local waters.

Complexities in spatial distribution are important to sampling design for chlorophyll mapping and flux measurements. Real-time aerial observation is obviously necessary for selection of sampling sites representative of the extant range of cell densities, unless surface sampling can be dense and widespread. Even continuous-flow fluorometry data used for chlorophyll fluctuation analysis (Platt, 1972; Lekan and Wilson, 1978) can fail to be representative when obtained from such complex and rapidly-changing patterns. Aerial photography and other imaging types of remote sensing coordinated with field sampling provide permanent records for later analysis of surface sampling and for mapping the spatial dimensions of the bloom.

PHOTO CALIBRATION AND VOLUME REFLECTANCE

Photography is subject to variable factors affecting emulsion densities which are independent of the water content (Bressette, 1977; Scarpace, 1978). These include water surface and bottom reflections, solar zenith angle, atmospheric path radiance, camera vignetting (which bent the scans in Figure 3), and overlap of dye spectra in film emulsion layers. Corrections for these variables are required for quantitative mapping of cell density or chlorophyll concentration values.

In the turbid York River, bottom reflections are insignificant except at the shoreline. The photographs were obtained at low altitude on clear days, making the impact of atmospheric variations negligible. The impact of surface reflections is negligible except in areas of sun glint (see Figure 2).

Beyond these difficulties unrelated to water content, there remain problems related to water content, which in turbid estuaries confuse the interpretation of remote sensing data. The signifi-

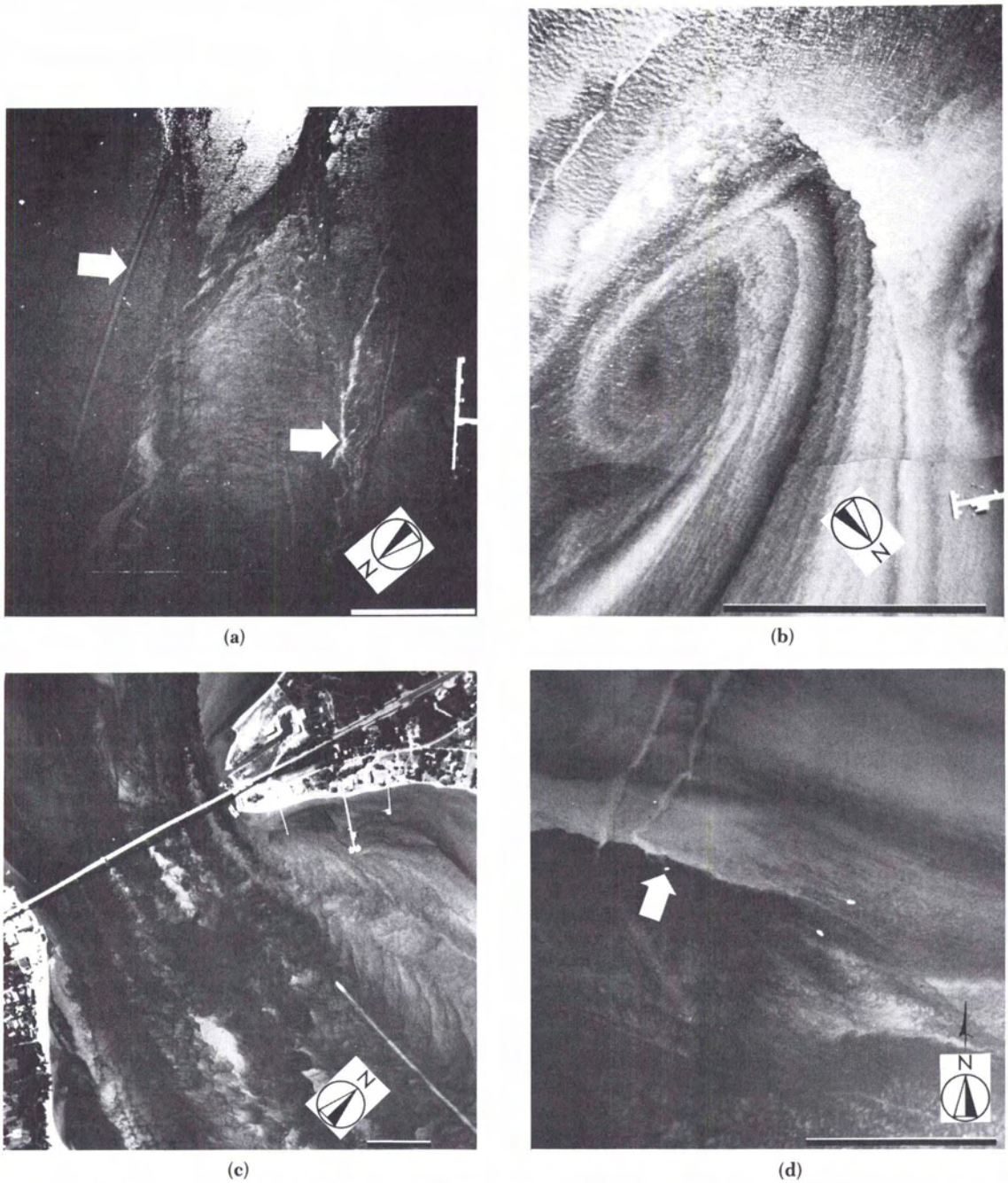

(a) (b)

(c) (d)

FIG. 2. Panchromatic copies of color photography of York River, Virginia dinoflagellate blooms. Scale bar in lower right of each photo indicates 300 m. Hasselblad 70-mm format. (a) Original Aerochrome Infrared 2443; red filter used in copying. One white arrow points to a zone colored pink on the original image, the other to a recent boat wake. (b) A large gyre near the VIMS pier. Original Hi-Speed Ektachrome. (c) Gloucester Point with VIMS at the upper right. Note the long-distance effect of bridge pilings. Bridge length over water is 820 m. Original Hi-Speed Ektachrome. (d) The white arrow marks a vessel sampling 1038 μg/l chlorophyll *a*. The chlorophyll *a* concentration of the adjacent "clear" water was 99 μg/l. Original Hi-Speed Ektachrome.

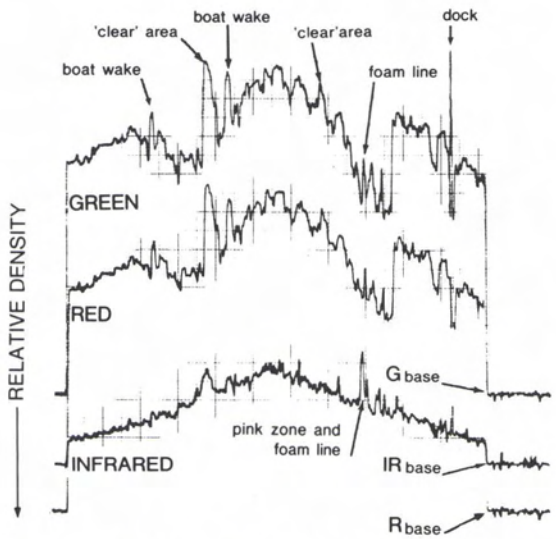

FIG. 3. Microdensitometer color-separation scans of color-infrared frame shown in Figure 2a. The edge-to-edge distance covers 1.25 km. The scan crossed the image horizontally at the lower white arrow.

cant parameter for remote sensing is volume diffuse reflectance. Models of diffuse reflectance, R, have the form

$$R = k\frac{b/a}{1 + b/a} = \frac{kB\,\omega_o}{1 - F\,\omega_o} \qquad (1)$$

where k is a constant, b the backscattering coefficient, a the absorption coefficient, B and F ($\equiv$ 1-B) are the fractions of forward, F, and backscattered, B, light, and ω_0 is the single-scattering albedo $\omega_0 = \underline{b}/\underline{b} + a$), where $\underline{b}$ is the total scattering coefficient (from which $b = \underline{b}B$) (Gordon *et al.*, 1975; Duntley *et al.*, 1974; Morel and Prieur, 1977). Equation 1 is a very close approximation to detailed solutions of the radiative transfer equation for $\omega_0 < 0.8$ (Gordon, 1973; McCluney, 1974; Jain and Miller, 1977). The ω_0 constraint will generally be satisfied in estuarine phytoplankton blooms because of large values of a. Using Equation 1, Gordon (1977) emphasized that a remote sensing technique (presumed to involvé a single spectral band) can provide information only on the ratio b/a. It follows that, if different components contribute to b and a, and their concentrations vary independently, measurement of the concentration of any one component from single band data will be impossible, and the interpretation of R will be ambiguous.

The possibility of confusion is illustrated here by the infrared scan in Figure 3, where cell concentration increases are associated with both reflectance increase and decrease. Thorne (1977) and Scherz (1977), in laboratory measurements of single algal species, report that reflectance at absorption maxima first increases and then decreases with increasing chlorophyll concentration. Equation 1 does not allow such reversals (see the discussion at Equation 11 below), and *in vivo* red absorption bands (see Figure 1) fall under the red photographic band, not the infrared. Therefore, we looked for causes other than reversals suggested by laboratory results, and we ascribe equivocal reflectance changes to simultaneous variations in dinoflagellate and inorganic suspended sediment concentrations as a function of depth.

By inspection, Equation 1 indicates that, for a background level of inorganic suspended solids, S_i, causing scattering but negligible absorption, the addition of highly absorbing dinoflagellates (with only weak scattering) will decrease upwelling radiance. During the photography, most S_i values were below 30 mg/l; this level produces approximately half the maximum possible upwelling red radiance (based on Landsat multispectral scanner (MSS) band 5 data with path radiance discounted). In the absence of blooms, C is approximately 10 μg/l, and b overshadows a. During blooms, C ranged from 50 to 1000 μg/l; at locations with pronounced image darkening, C was above 100 μg/l and produced organic S_0 of 20 to 40 mg/l. The high dinoflagellate concentrations contribute more to total absorption than total scattering in the visible region, resulting in observed reflectance decreases in the blue, green, and red bands.

In boat wakes, surface strata are disrupted by subsurface waters containing greater sediment loads and reduced dinoflagellate concentrations. Consequently, absorption in the visible bands decreases (because C decreases), scattering increases (because S increases), and therefore R increases. In the infrared band, where the absorbance of dinoflagellates is negligible (the tail of chlorophyll absorption extends only to 720 nm), the phytoplankton contribution to scattering is reduced by disruption of surface strata, yet compensated for by a higher sediment load. The result is still an increase in R.

In the pink zones of extremely high cell density, however, an increase in the infrared scattering due to accumulation of cells in the surface layer (<1 optical depth) can more than compensate for the slow settling out of sediment, and the infrared R again increases.

Thus, equivocal reflectance changes can result from simultaneous variations in the depth profile of cell concentrations and inorganic suspended sediment. The data indicate that the infrared band is more sensitive to this problem than the visible bands (due to the greater absorbance of water in the infrared). Therefore, in turbid waters, color photography may be better than color infrared for bloom detection.

AMBIGUOUS INTERPRETATIONS FROM CONSTANT REFLECTANCE

At some wavelengths, which depend on the spectral variations in scattering and absorption, it

is possible for R to be invariant (see Figure 6 of Morel and Prieur, 1977) even though both cell concentration and sediment load are changing. The condition for invariant R can be obtained from Equation 1 by taking

$$dR = [k/(a + b)^2]\,[adb - bda] = 0. \quad (2)$$

The dependence of R on B and F is not considered here because, at any given stage of a bloom, a spatial variation in B and F is very unlikely. Equation 2 yields

$$db/da = b/a \text{ or } db/b = da/a. \quad (3)$$

For any number n of components i, each with concentration x_i, let

$$b = \sum_i^n b_i = \sum_i^n b'_i x_i \quad (4)$$

and similarly for a, where b'_i is the specific backscattering coefficient. The condition

$$dx_1/x_1 = dx_2/x_2 = \ldots = dx_n/x_n \quad (5)$$

produces $dR = 0$, because by

$$db = \sum_i^n db_i = \sum_i^n b'_i dx_i = \sum_i^n b'_i x_i (dx_n/x_n)$$

$$= (dx_n/x_n) \sum_i^n b'_i x_i, \quad (6)$$

and a similar result for da, the ratio db/da is still equal to b/a.

The particular invariance condition of Equation 5 cannot be rigorously realized because the water coefficients, b_w and a_w, although wavelength dependent, are constant. However, with only two particulate components, S and C, in estuarine waters, Equation 1 can be re-expressed as

$$R = k(b_w + b_s + b_c)/(a_w + a_y + a_s + a_c + b_w + b_s + b_c) \quad (7)$$

where the subscripts y, s, and c refer to dissolved pigments, sediment, and chlorophyll particles, respectively. From Equation 4, let $b_s = b'_s S$, and similarly for a_s, b_c, and a_c. Then, if both S and C vary, $dR = 0$ yields

$$\frac{dC}{dS} = \frac{a'_s b_w - b'_s(a_w + a_y) + C(a'_s b'_c - b'_s a'_c)}{b'_c(a_w + a_y) - a'_c b_w + S(a'_s b'_c - b'_s a'_c)} \quad (8)$$

This expression approaches Equation 5 in the limit of increasing C and S, where $dC/dS = C/S$. For $C = 50$ µg/l and $S = 10$ mg/l, and the coefficient values of Table 1, $dC/dS = 7.7$ at 680 nm, but -24 at 700 nm. Such numbers from Equation 8 provide a measure of the "resolving power" of different wavelengths for the components C and S. The numbers indicate that dS more easily overwhelms dC at 700 than at 680 nm. Therefore, 680 nm is the better wavelength for chlorophyll detection in the presence of varying S.

TABLE 1. COEFFICIENTS FOR REFLECTANCE MODEL SIMULATIONS IN FIGURE 4

Coefficient	680 nm	700 nm	Reference
k	0.33	0.33	M&P
b_w (m^{-1})	0.0003	0.00025	M&P
a_w (m^{-1})	0.450	0.650	M&P
a_y (m^{-1})	0.0026	0.0019	J
a_c' ($m^{-1} * C^{-1}$)	0.02	0.002	W&K
b_c' ($m^{-1} * C^{-1}$)	0.0030	0.0027	W&K
a_s' ($m^{-1} * S^{-1}$)	0.01	0.01	*
b_s' ($m^{-1} * S^{-1}$)	0.03	0.0291	*

C chlorophyll a in µg/l.
S suspended sediment in mg/l.
* b_s (680 nm) set to yield roughly $R_{max} = 0.24$. λ^{-1} dependence. a_s then set to yield roughly half R_{max} at $S = 30$ (from Landsat data; see text).

J Jerlov, 1968.
M&P Morel and Prieur, 1977.
W&K Wilson and Kiefer, 1979.

Invariant R can also result when either C or S is sufficiently large. If C is constant, $dR/dS = 0$ yields

$$C = \frac{a'_s b_w - b'_s a_w - a_y b'_s}{b'_s a'_c - a'_s b'_c} \quad (9)$$

and invariant R takes the limiting value

$$R_{max} = kb'_s/(a'_s + b'_s). \quad (10)$$

Only positive C values from Equation 9 are meaningful. In the visible and infrared bands, $a_w > b_w$, and usually $b'_s > a'_s$. Therefore, positive C requires that $b'_c/a'_c > b'_s/a'_s$. Thus, component C would have to be as strong a scatterer relative to its absorption as component S. In the green and infrared bands, phytoplankton cells might meet this constraint. For the values of Table 1 at 700 nm, $R_{max} = 0.24$.

For laboratory unialgal cultures, invariant R is obtained if the algal coefficients b'_c and a'_c obey

$$b'_c/a'_c = b_w/a_w. \quad (11)$$

Note that Equation 11 is independent of C, which rules out reversals of R with increasing C. Because the various coefficients vary with wavelength, the condition (11) produces for spectral reflectance curves calculated for different unialgal concentrations what Duntley *et al.* (1974) term a "hinge point" (see also Wilson and Keifer, 1979). Note that, although R is constant at the hinge point, optical depth is not. Also, from available values for a'_c, b_w, and a_w at the hinge point, Equation 11 provides a measure of b'_c, useful when b'_c data are not available.

Similarly, in sediment-laden waters with negligible phytoplankton and $a_y = 0$, invariant R would be obtained if

$$b'_s/a'_s = b_w/a_w. \quad (12)$$

ANALYSIS USING THE REFLECTANCE MODEL

There is not yet enough spectral information available for a complete analysis of the film data using the model. However, patterns produced by the model can be seen in Figure 4, where reflectance is predicted as a function of sediment content with chlorophyll concentration as a parameter. Values used for the coefficients in Equation 7 are shown in Table 1. The red absorption band of chlorophyll (680 nm) is simulated in Figure 4a. The reflectance diminishes with increasing C as observed in the photographic red band. The near infrared border region (700 nm) where chlorophyll absorption is much less is simulated in Figure 4b. The sequence 1-3 illustrates equivocal reflectance changes with increasing C, as described earlier for the infrared band of the photography.

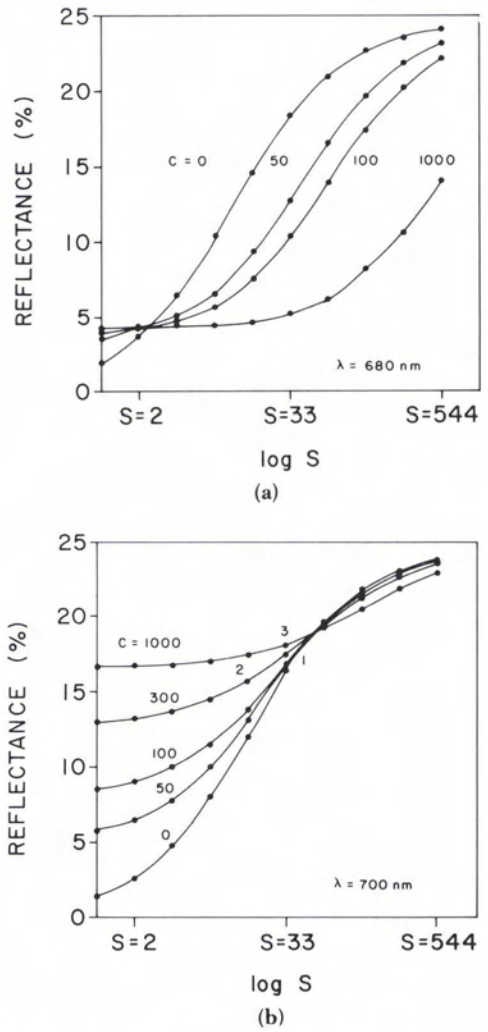

FIG. 4. Reflectance model simulations (Equation 7). Coefficient values are from Table 1. C = chlorophyll a in μg/l; S = sediment in mg/l. (a) 680 nm. (b) 700 nm. In the sequence 1-3, as C increases, R decreases, then increases.

DISCUSSION

The analysis shows that, in estuarine waters with two or more types of components, invariant reflectance will result when concentrations undergo proportional changes or when one constant-level component masks another. Generally, small changes in R within a single spectral band will have an ambiguous interpretation when more than one component is varying. Consequently, for remote sensing to have universal power in estuaries for accurate measurement of types of phytoplankton and sediment, the optical properties of estuarine waters must be well-known and capable of simple modeling, and/or a multispectral technique must be available. A multispectral technique must be spectrally very selective to resolve even a small number of components. If the components are similar spectrally, only broad classes of components may be distinguishable. Some airborne multispectral systems are presently available which may have sufficient selectivity for the conditions of turbid estuaries (see Miller *et al.* (1976) and Grew (1977) for examples of aerial rapidscan spectroradiometer data which may be suitable). For satellites, the Coastal Zone Color Scanner (CZCS) on Nimbus 7 has better spectral channels than the broad band multispectral scanner on Landsat, but the CZCS spatial resolution is too poor for most estuarine study (800 m for CZCS compared to 80 m for Landsat).

Despite the lack of enough basic optical data, and barely adequate sensors, there has been success in making accurate measurements of gross chlorophyll and sediment concentrations in turbid waters using widely available remote sensing data (Munday and Alföldi (1979), and Munday *et al.* (1979) and references therein). This demonstrates that turbid waters often display spectral simplicity for wide spectral bands despite mixtures of various absorbing and scattering components. Likewise, the photography illustrated here shows that, during several summer dinoflagellate blooms dominated by single species, areal distributions in local waters have been portrayed with the simple technique of color and color-infrared photography.

The general conclusion follows that remote measurement of phytoplankton and sediment components in turbid estuaries is possible, but results from particular study areas cannot yet be

generalized to other areas. Further work on optical properties of estuaries and on mixture analysis of components using reflectance models is needed. The results of such efforts may ultimately be useful in ecosystem flux analysis and environmental impact evaluation.

With the above background, we have reconsidered well-known turbidity variations seen on Landsat imagery and NASA photography of local waters. A prevailing view is that areas of low reflectance found in river channels and the center of large bays represent low sediment loads, and that nearshore scouring produces higher sediment loads and higher reflectance values in nearshore zones (Klemas *et al.*, 1973). However, York River dinoflagellate blooms are usually of greatest density in the mid-river channel. Because blooms generally cause a reflectance decrease in turbid waters, they would be relatively indistinguishable from low sediment loads in imagery of poor spatial and spectral resolution. In imagery of high spatial resolution, blooms might be distinguished by their image texture, because motile dinoflagellate distributions are more complex than sediment distributions. Also, in our experience, blooms have had sharper concentration gradients. Landsat 3 lacks sufficient spatial resolution to distinguish phytoplankton from sediment patterns by means of texture, but has enough spectral selectivity if the cell concentrations are high (Alföldi and Munday, 1978; Munday *et al.*, 1979). Conversely, if chlorophyll concentrations are below 30 to 50 μg/l, the infrared band threshold of detection according to Bressette and Lear (1973), and sediment is the dominate cause of turbidity (the case for Chesapeake Bay, as shown by Bowker *et al.* (1977) then historical Landsat data are useful for accurate mapping of estuarine surface sediment loads. Such mapping of sediment loads has importance in engineering and hydrodynamic studies (Amos and Alföldi, 1979; Munday *et al.*, 1979).

Acknowledgments

We deeply appreciate the assistance of J. E. Warinner III and L. Shem who aided with sample analysis, C. Alston for aerial photography, R. Adams (NASA Langley) who assisted with the microdensitometry, and E. Ferraz-Reyes (Instituto Oceanografica, Cumaná, Venezuela) who identified phytoplankton. The manuscript was typed by L. Marshall.

References

Alföldi, T. T., and J. C. Munday, Jr., 1978. Water quality analysis by digital chromaticity mapping of Landsat data. *Canadian J. Remote Sensing* 4(2): 108-126.

Amos, C. L., and T. T. Alföldi, 1979. The determination of suspended sediment concentration in a macrotidal system using Landsat data. *J. Sedim Petrol.* 49(1):159-174.

Bowker, D. E., W. G. Witte, P. Fleischer, T. A. Gosink, W. J. Hanna, and J. C. Ludwick, 1975. An investigation of the waters in the lower Chesapeake Bay area. *Proc. 10th Intl. Symp. Remote Sensing of Environment*, Env. Res. Inst. Michigan, pp. 411-420.

Bressette, W. E., 1973. The use of near infrared photography for aerial observation of phytoplankton blooms. In *Remote Sensing of Earth Resources*, Vol. II, Univ. Tennessee Space Inst., pp. 1173-1186.

———, 1977. Effect of detector threshold, location of the sun and flight altitude upon spectral variations in remote sensing over water. In *Remote Sensing of Earth Resources*, Vol. VI, Univ. Tennessee Space Inst., pp. 67-88.

Bressette, W. E., and D. E. Lear, Jr., 1973. The use of near-infrared reflected sunlight for biodegradable pollution monitoring. EPA 2*nd* Env. Quality Sensors Conf., Las Vegas.

Bukata, R. P., G. P. Harris, and J. E. Bruton, 1974. The detection of suspended solids and chlorophyll *a* utilizing digital multispectral ERTS-1 data. *2nd Canadian Symp. Remote Sensing*, Guelph, Ontario, Canadian Remote Sensing Society, Ottawa, Canada, pp. 552-564.

Duntley, S. Q., R. W. Austin, W. H. Wilson, C. F. Edgerton, and S. E. Morgan, 1974. *Ocean color analysis.* Scripps Inst. Oceanogr. Ref. 74-10, sep. p.

Gordon, H. R., 1973. Simple calculation of the diffuse reflectance of the ocean. *Appl. Opt.* 12:2804-2805.

———, 1977. One-parameter characterization of the ocean's inherent optical properties for remote sensing. *Appl. Opt.* 16(1):2627.

Gordon, H. R., and O. B. Brown, 1973. Irradiance reflectivity of a flat ocean as a function of its optical properties. *Appl. Opt.* 12:1549-1551.

Gordon, H. R., O. B. Brown, and M. M. Jacobs, 1975. Computed relationships between the inherent and apparent optical properties of a flat homogeneous ocean. *Appl. Opt.* 14:417-427.

Govindjee, 1960. Letter. *Biophysical J.* 1(4):373-375.

Grew, G., 1977. Characteristic vector analysis as a technique for signature extraction of remote ocean color data. In *Remote Sensing of Earth Resources*, Vol. VI, Univ. Tennessee Space Inst., p. 109-144.

Haas, L., 1977. The effect of the spring-neap tidal cycle on the vertical salinity structure of the James, York and Rappahannock Rivers, Virginia, U.S.A. *Estuar. Coast. Mar. Sci.* 5:485-496.

Jain, S. C., and J. R. Miller, 1977. Algebraic expression for the diffuse irradiance reflectivity of water from the two-flow model. *Appl. Opt.* 16:202-204.

Jerlov, N. G., 1968. *Optical oceanography.* Elsevier.

Klemas, V., M. Otley, and C. Wethe, 1973. Monitoring coastal water properties and current circulation with ERTS-1. *Third ERTS-1 Symposium*, NASA, Washington, D.C., pp. 1387-1411.

Lekan, J. F., and R. E. Wilson, 1978. Spatial variability of phytoplankton biomass in the surface waters of Long Island. *Estuar. Coast. Mar. Sci.* 6(3):239-251.

McCluney, W. R., 1974. Ocean color spectrum calculations. *Appl. Opt.* 13:2422-2429.

McNeil, W. R., K. P. B. Thomson, and J. Jerome, 1976. The application of remote spectral measurements to water quality monitoring. *Canadian Jour. Remote Sensing* 2:48-58.

Miller, J. R., K. S. Gordon, and D. Kamykowski, 1976. Air-borne water-colour measurements off the Nova Scotia coast. *Canadian Jour. Remote Sensing* 2(1):42-47.

Morel, A., and L. Prieur, 1977. Analysis of variations in ocean color. *Limnol. Oceanogr.* 22:709-722.

Mueller, J. L., 1973. *The influence of phytoplankton on ocean color spectra.* Ph.D. Thesis, Oregon State Univ.

Munday, J. C., and T. T. Alföldi. 1979. Landsat test of diffuse reflectance models for aquatic suspended solids measurement. *Remote Sens. Env.* 8:169-183.

Munday, J. C., Jr., T. T. Alföldi, and C. L. Amos, 1979. Bay of Fundy verification of a system for multidate Landsat measurement of suspended sediment. In *Satellite Hydrology, Proc. 5th Annual William T. Pecora Memorial Symp.*, Sioux Falls, South Dakota, 35 p., in press.

Platt, T., 1972. Local phytoplankton abundance and turbulence. *Deep Sea Research* 19:183-187.

Scarpace, F. L., 1978. Densitometry on multi-emulsion imagery. *Photogr. Eng. Remote Sensing* 44(10): 1279-1292.

Scherz, J. P. (ed.), 1977. *Assessment of aquatic environment by remote sensing.* Inst. Env. St., Univ. Wisconsin, 235 p.

Strickland, J. D., and T. R. Parsons, 1972. *A practical handbook of seawater analysis*, 2nd Ed. Bull. Fish. Res. Bd. Can. 167, 310 p.

Thorne, J. F., 1977. The remote sensing of algae. In *Remote Sensing of Earth Resources*, Vol. VI, Univ. Tennessee Space Inst., pp. 145-160.

Tyler, M. S., and H. H. Seliger, 1978. Annual subsurface transport of a red tide dinoflagellate to its bloom area: Water circulation patterns and organism distributions in the Chesapeake Bay. *Limnol. Oceanogr.* 23(2):227-246.

Wilson, W. H., and D. A. Kiefer, 1979. Reflectance spectroscopy of marine phytoplankton. Part 2. A simple model of ocean color. *Limnol. Oceanogr.* 24(4):673-682.

Zubkoff, P. L., J. C. Munday, Jr., R. G. Rhodes, and J. E. Warinner, 1979. Mesoscale features of summer (1975-1977) dinoflagellate blooms in the York River, Virginia (Chesapeake Bay estuary). In *Toxic Dinoflagellate Blooms, Proc. 2nd Intl. Conf.*, Elsevier/ North-Holland, New York, pp. 279-286.

Zubkoff, P. L., and J. E. Warinner III, 1975. Synoptic sightings of red waters of the lower Chesapeake Bay and its tributary rivers. (May 1973-September 1974). In *Toxic Dinoflagellate Blooms, Proc. 1st Intl. Conf.*, Mass. Sci. Tech. Foundation, Wakefield, Mass., pp. 105-111.

———, 1976. The effect of tropical storm Agnes as reflected in chlorophyll *a* and heterotrophic potential of the lower Chesapeake Bay. In *The Effects of Tropical Storm Agnes on the Chesapeake Bay Estuarine System*, Johns Hopkins Univ. Press, CRC Publication No. 54, pp. 368-388.

(Received 5 April 1980; revised and accepted 4 October 1980)

Workshop on Automated Photogrammetry and Graphics in Highways and Transport

Red Lion Motor Inn
Portland, Oregon
28 April through 1 May 1981

This workshop, sponsored by the American Society of Photogrammetry, will include, in addition to two panel discussions on Computer Aided Design, the following sessions:

- Digital Terrain Models
- Close Range Applications
- Automated Systems
- Special Techniques
- Computer Graphics and Design

For further information please contact

Columbia River Region—ASP—
Emery Ullom, Registration Chairman
502B E. 29th Street
Vancouver, WA 98663